

PCCP

Accepted Manuscript



This is an *Accepted Manuscript*, which has been through the Royal Society of Chemistry peer review process and has been accepted for publication.

Accepted Manuscripts are published online shortly after acceptance, before technical editing, formatting and proof reading. Using this free service, authors can make their results available to the community, in citable form, before we publish the edited article. We will replace this *Accepted Manuscript* with the edited and formatted *Advance Article* as soon as it is available.

You can find more information about *Accepted Manuscripts* in the [Information for Authors](#).

Please note that technical editing may introduce minor changes to the text and/or graphics, which may alter content. The journal's standard [Terms & Conditions](#) and the [Ethical guidelines](#) still apply. In no event shall the Royal Society of Chemistry be held responsible for any errors or omissions in this *Accepted Manuscript* or any consequences arising from the use of any information it contains.

High performance surface-enhanced Raman scattering from molecular imprinting polymers capsulated silver spheres

Cite this: DOI: 10.1039/x0xx00000x

Yan Guo,^a Leilei Kang,^a Shaona Chen^a and Xin Li^{*b,a}

Received 00th January 2014,
Accepted 00th January 2014

DOI: 10.1039/x0xx00000x

www.rsc.org/

Driven by the ultrasensitivity of surface-enhanced Raman scattering (SERS) technique and the directive selection of molecular imprinting polymers (MIPs), core-shell silver-molecularly imprinted polymers (Ag@MIPs) hybrid structure was synthesized to serve as a novel SERS platform. The results show that as prepared Ag@MIPs wrapping over a thin shell of MIPs is sensitive to the template molecule (Rhodamine 6G). To investigate the selectivity of Ag@MIPs, the structurally related molecules, such as Rhodamine B and crystal violet, were chosen as controls. Notably, the high sensitivity of Ag@MIPs is restrained by the non-specific recognition of Rhodamine B and crystal violet. This high SERS enhancement for template molecule can be interpreted by “gate effect” and/or “dummy hot spots”. We believe that the sensitivity of SERS coupled with the selectivity of MIPs could induce a promising chemosensor or biosensor for practical applications.

Introduction

Surface-enhanced Raman scattering (SERS) has witnessed a tremendous advance in theoretical and experimental results as the rapid development of computational science and nanotechnology since this available phenomenon was discovered in 1974.^{1, 2} Based on SERS method, the detection limit has achieved an unprecedented level, single molecule detection.³⁻⁶ Besides scientific research, a great deal of efforts has been made in order to apply this promising tool to our real life, such as food,^{7, 8} environment,⁹ medicine,^{10, 11} and so on.^{12, 13} To meet these demands, all kinds of SERS substrates with superhydrophobicity,¹⁴ high affinity¹⁵ and intense plasmonic nanostructures¹⁶ have been fabricated in the recent years. However, it is still a challenge for these developed SERS platforms to fulfil the requirements relevant to significant social problems.^{17, 18}

Molecular imprinting technique (MIT) has been developed as one of the most important tools for the specific identification, separation and analyte detection in chemistry, biology, materials, and medicine.¹⁹⁻²³ Taking the advantages of stabilization, specific recognition and reusability, molecular imprinting polymers (MIPs) is of great interest. Hence, the combination of the advantages of SERS and MIPs would be expected to immensely promote the development of sensitive and selective detection. However, the number of reported papers relevant to the marriage of SERS and MIPs is very limited to date. MIPs were

explored to integrate with a SERS-active film as the sensing layer to detect the explosive, 2,4,6-trinitrotoluene (TNT)²⁴. A SERS-based sensor for the determination of theophylline had been developed by imprinting the template molecules on the SERS active surface of Ag nanoparticles, showing a good reproducibility and a dose-response relationship.²⁵ Long and coworkers reported that surface-imprinted core-shell Au nanoparticles can be explored for highly selective detection of bisphenol A (BPA) based on SERS. The detection limit can reach 0.12 mg L⁻¹ owing to the obviously specific identification, which furnishes a promising tool to sensitive and selective detection in real samples.²⁶ Recently, we have reported that the core-shell silver-molecularly imprinted polymers (Ag@MIPs) hybrid as SERS platform is potential for ultrasensitive sensing and analytical applications.²⁷

Here, we introduce the synthesis of Ag@MIPs hybrid system using Rhodamine 6G (R6G) as the template molecule. The developed Ag@MIPs complex is sensitive to the template molecule due to the specific recognition. Moreover, the ability of its exclusively selective detection of R6G was carefully investigated by comparing with other analogues, such as Rhodamine B (RB) and Crystal violet (CV).

Experimental

Synthesis of Ag microspheres. Ag particles were synthesized by integrating of the reported methods with some improve-

ments.^{28, 29} In a typical liquid-phase reduction synthesis, 2 mL of AgNO₃ aqueous solution (1 M) and 20 mL of poly vinyl pyrrolidone aqueous solution (0.2 M, $M_w \approx 40000-50000$) were added into 100 mL of ultrapure water with stirring in an ice-water bath. Then, 2 mL of ascorbic acid (1 M) was quickly injected into mixture and stirred continually for 15 min. The resulting products were collected by centrifugation and then dried in vacuum at 40 °C for 24 h.

Synthesis of Ag@MIPs hybrid. To modify the surface of Ag particles with 3-methacryloxypropyltrimethoxysilane (MPS), 500 mg of Ag particles and 8 mL of MPS were added into 40 mL solution of ethanol-water (4:1, v/v). After the sample dissolved completely, the mixture was magnetic stirred at 40 °C for 24 h under nitrogen protection. The products (Ag@MPS) was washed with ethanol for several times and then dried under vacuum. In order to synthesize Ag@MIPs hybrid, 0.5 mmol of R6G, 5 mmol of acrylamide, 25 mmol of ethylene glycol dimethacrylate (EGDMA), 20 mg of azobisisobutyronitrile (AIBN) and 200 mg of modified Ag particles (Ag@MPS) were dispersed into 40 mL of acetonitrile and stirred 24 h at 65 °C under the protection of nitrogen. The sample was washed with methanol-acetic acid (4:1, V/V) solution until no template molecule was detected in the washing solution by UV-vis spectroscopy. Finally, the resulting products were washed with ethanol and then dried under vacuum at 40 °C for 24 h.

Characterization. The products were characterized by X-ray diffractometer (XRD, Shimadzu XRD, 6000) with Cu K α radiation ($\lambda = 1.5418 \text{ \AA}$), transmission electron microscope (TEM, FEI, Tecnai G² F20), and scanning electron microscopy (SEM, Hitachi S4800 HSD). Fourier transform infrared spectra (FT-IR) were recorded on an Avatar 360 (Nicolet) instrument by dispersing the sample in a KBr pellet (0.1%, w/w). UV-vis absorption spectra were conducted on T6 (Beijing Purkinje General Instrument Co.,Ltd). SERS spectra were collected on a Renishaw inVia confocal micro-Raman spectroscopy system ($\lambda = 633 \text{ nm}$). The incident laser power and exposure time was kept at 0.1 mW and 10 s, respectively.

Results and discussion

The detection of specific and low-affinity molecules is one of the problems need to be urgently solved in SERS field. Polymers resulted from the polymerization of monomers retain populations of complementary matching sites in the presence of target molecules or a fragment due to the collective interactions between monomers and templates, which provides a possible way to overcome the drawbacks of SERS technology.²³ In our previous work, we have successfully synthesized Ag@MIPs hybrid with high sensitivity.²⁷ However, its selectivity has not yet been investigated. It is well-known that SERS phenomenon is an obvious surface effect. Especially for core-shell structure, the shell thickness is considered to be the key factor that affects SERS performance and the Raman signal decreases exponentially with increasing shell thickness.^{30, 31} Therefore, the fabrication of Ag@MIPs with thin MIPs should be beneficial to improving SERS performance. We herein prepared Ag@MIPs

residing short-distance recognition sites onto Ag core. Schematic illustration of the fabrication and detection process of Ag@MIPs is presented in Fig. 1.

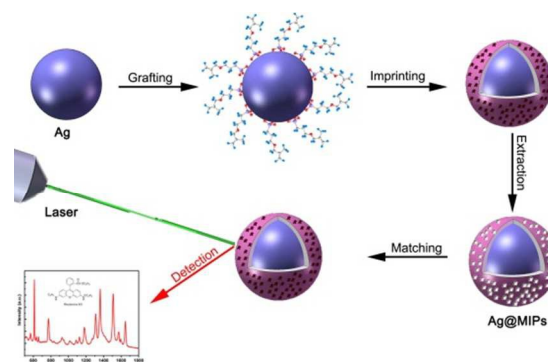


Fig. 1 schematic illustration of the fabrication and detection process of Ag@MIPs.

As shown in Fig. 2, SEM and TEM images were conducted to evaluate the morphology and nanostructures of Ag and Ag@MIPs. Ag particles with smooth surface were produced, which would be harmful to SERS response, but offer a good opportunity to wrap a uniform shell of MIPs. And the distribution of particle size is narrowed to $\sim 800 \text{ nm}$ in diameter (Fig. 2a). There is no obvious changes in surface morphology between Ag and Ag@MIPs spheres, except for a small amount of scattering aggregates which possibly come from the self-polymerization of functional monomers (Fig. 2c). Compared with TEM image of Ag spheres, a shell with a thickness of about 16 nm clearly appears on the Ag@MIPs surface, indicating that Ag spheres have been successfully encapsulated by MIPs (Fig. 2b and d). It is worthy to point out that the self-polymerization of monomer is inevitable in the polymerization process, which slightly disturbs the quality of MIPs shell.

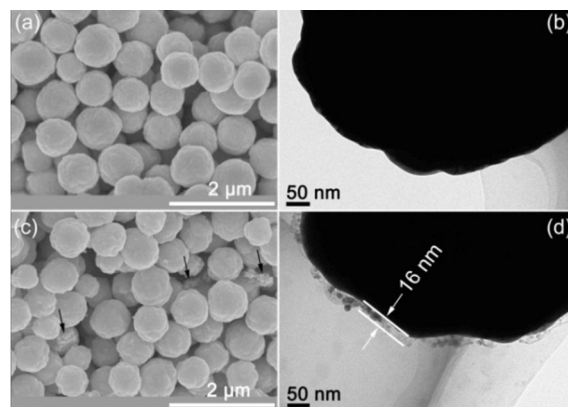


Fig. 2 SEM and TEM images of Ag spheres (a, b) and Ag@MIPs (c, d). Arrows pointed scattering aggregates originated from the self-polymerization of functional monomer.

X-ray diffraction (XRD) patterns of Ag and Ag@MIPs in Fig. 3 show the typical face-centered cubic (fcc) Ag crystal phase, where the diffraction peaks can be well indexed to the (111), (200), (220) and (311) crystal planes. The relative intensity ratio of diffraction peaks are almost identical but the corre-

sponding peak intensity of Ag@MIPs is weaker than that of pure Ag phase, suggesting that the encapsulation process would impair the intensity of diffraction peaks. Furthermore, the energy dispersive spectrum (EDS) from Ag@MIPs shows the existence of C and O which is absent from that of naked Ag spheres (Fig. S1). Also, there are lots of newly formed functional groups in fourier transform infrared (FT-IR) spectrum collected from Ag@MIPs. The detailed analysis shows that these vibrational modes come from functional monomer (acrylamide) and cross linking agent (EGDMA) (Fig. S2). These data, taken together, indicate that MIPs has been successfully wrapped over the Ag cores.

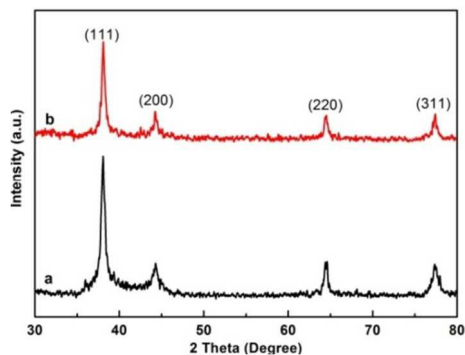


Fig. 3 XRD patterns of Ag (a) and Ag@MIPs (b).

The removal of template molecules is one of the most important procedures to realize the quantitative determination of target molecules for MIPs. Fig. 4 shows the UV-visible absorption spectra of R6G in supernatant liquid as a function of cleaning time scale. It can be seen that the initially prominent absorption peak gradually declines as the washing process continues, and completely disappears after 4 h, which manifests that R6G molecules have been thoroughly eliminated from Ag@MIPs. The weak and ambiguous Raman peaks collected from washed Ag@MIPs demonstrate that these formerly imprinted recognition sites on MIPs were created after a long period of washing time (Fig. S3).

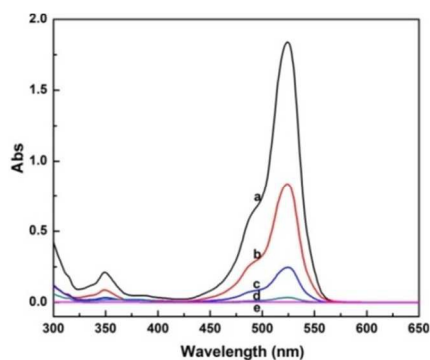


Fig. 4 UV-visible spectra of R6G in supernatant liquid as a function of rinse time scale of (a) 0 h, (b) 1 h, (c) 2 h, (d) 3 h and (e) 4 h.

R6G, template molecule in our system, was used as the first target analyte to examine the SERS performance of the prepared Ag@MIPs. As shown in Fig. S4, Raman spectra of R6G at a concentration of 10^{-5} M were collected from Ag particles and Ag@MIPs, respectively. It can be seen that high-quality

Raman spectra of R6G were obtained. The characteristic Raman fingerprints of R6G molecules at 1313 cm^{-1} , 1360 cm^{-1} , 1508 cm^{-1} , 1570 cm^{-1} and 1648 cm^{-1} can be assigned to C=C stretching vibration of benzene ring. And a prominent peak at 611 cm^{-1} is responsible for C-C resonance. Moreover, Raman bands at 774 cm^{-1} and 1184 cm^{-1} can be ascribed to stretching and bend vibration of C-H. These peak positions are well consistent with the reported works employing R6G as the model analyte.³²⁻³⁴ One can find that the corresponding Raman peaks collected from Ag@MIPs are much stronger than that from Ag spheres. This phenomenon indicates that recognition sites residing on Ag@MIPs could be more efficient as so called “hot spots” than gaps between pure Ag particles. The presence of MIPs avoids the target molecules directly contacting with plasmonic metal, which protects SERS active core from contaminating by what is being probed.

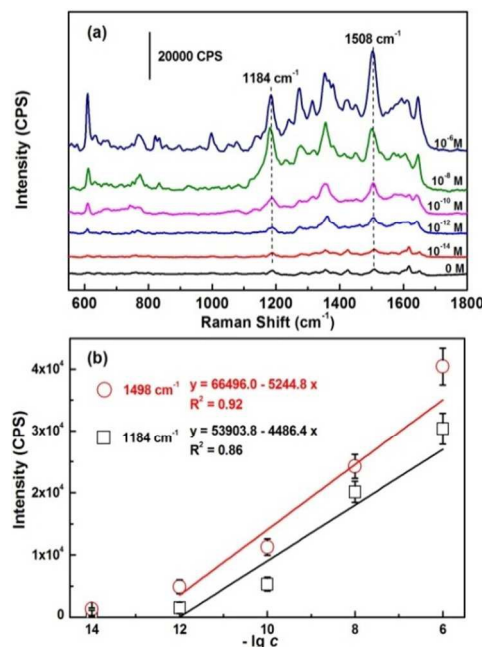


Fig. 5 (a) Concentration-dependent SERS spectra of R6G obtained from Ag@MIPs. (b) Linear relationship of Raman intensity as a function of R6G concentration for the bands at 1184 cm^{-1} and 1508 cm^{-1} . Each data point is the average result of three SERS spectra.

Concentration-dependent SERS spectra were recorded to test the SERS performance of Ag@MIPs by ascertaining the limit of detection. As shown in Fig. 5a, the intensity of characteristic peaks decline with decreasing the concentration of R6G. However, the distinguishable Raman fingerprints can still be clearly observed even the concentration of R6G was diluted to 10^{-14} M. Fig. 5b shows the plots of SERS intensity depending on the Raman peaks at 1184 cm^{-1} and 1508 cm^{-1} as a function of the concentration of R6G. Of note is that the SERS intensity is obtained by subtracting that of the blank sample. One can see that SERS intensity increases gradually as the increment of the concentration of R6G. There is a linear relationship between SERS intensity and the concentration of R6G in the range from 10^{-12} M to 10^{-6} M. Based on the given linear equations, as pre-

pared Ag@MIPs can be explored for quantitative detection. Interestingly, the SERS intensity of R6G dose not drop linearly when the concentration of R6G is 10^{-14} M. This could be interpreted that the imprinted cavities could be high efficient to capture the template molecule even the number of the molecules is very limited. Bearing this in mind, the detection limit of Ag@MIPs for R6G can be estimated as 10^{-14} M. The enhancement factor (EF) was calculated to be $\sim 10^8$ using the R6G peak at 1184 cm^{-1} (ESI). However, Ag spheres without MIPs can only detect R6G with a concentration above 10^{-7} M. (Fig. S5).

The specific recognition is the most important properties for MIPs. After removal of the template molecules, the imprinted cavities with spatial characteristics and chemical functionality were created. As a consequence, template molecules with specific size and functional groups will be anchored into cavities by chemical bonding in the penetration process. RB and CV, possessing similar molecular structures with R6G, were selected for investigating the specific recognition of Ag@MIPs. The results show that almost identical SERS intensity of them were collected when Ag particles were utilized as SERS platforms (Fig. S6). As expected, it can be seen in Fig. 6 that the Raman signal of R6G on Ag@MIPs is much stronger than that of RB and CV. This phenomenon is rationalized that R6G molecules can be captured into the cavities of MIPs because of the compatibility of the size and bonding effect. The only difference between R6G and RB in the molecular formula is functional group. Therefore, the weak non-covalent and/or reversible covalent interactions between functional groups of RB and active sites of MIPs leads to an unstable state for RB in the R6G formed sites, which may be responsible for a subdued SERS response. Further analysis shows that Raman intensity of RB is stronger than that of CV, which would originate from the mismatch in both of the size and functional groups. These results suggest that the Raman signal of template molecule can be tremendously amplified on Ag@MIPs by the specific recognition. In contrast, the analytes mismatching in spatial characteristic and/or bonding effect will obtain weak SERS signals. Notably, the SERS signals of RB and CV cannot completely vanish from Raman spectra. Because SERS technique is a very sensitive tool even though a very small amount of analytes are non-specifically absorbed onto the surface of Ag@MIPs.

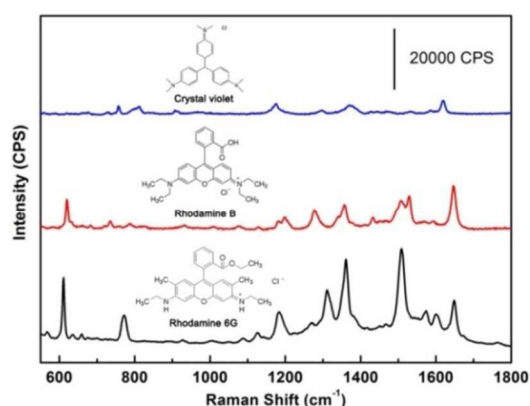


Fig. 6 SERS spectra of R6G, RB and CV recorded from Ag@MIPs at a concentration of 10^{-5} M and their corresponding molecular structures.

This sensitive and selective performance would be responsible for the core-shell structure and near-surface recognition sites. To date, charge transfer (chemical enhancement) and electromagnetic enhancement (physical enhancement) have been widely accepted as SERS enhancement mechanisms. However, the thickness of MIPs shell in our case is up to 16 nm, which is difficult to interpret by the classic theory (i.e. Förster resonance energy transfer).³⁵ The possible reason for MIPs based SERS mechanism is the existence of unobserved tunnel leading chemical species to the near surface of plasmonic metal, which is named “gate effect”.³⁶⁻³⁸ In our case, template molecule (R6G) will access to the cavities and close to the Ag core with the assistance of gate effect. It will be easy to understand that the high performance of Ag@MIPs is contributed by both of chemical and physical enhancement.

Recently, researchers found that laser light can be stored in a bottle-like microresonator for about ten nanoseconds. The interaction between light and single atoms will happen during this period.³⁹ Inspired by this phenomenon, we suggest that some of the recognition sites on MIPs can capture not only the spatial scale and/or chemical interaction matched species but also large amount of photons, which will be available “dummy hot spots” for SERS enhancement. Once matched species were anchored into these cavities, the Raman signals will be immensely amplified. But mismatch of species in size and chemical bonding will lead to a bleak SERS response. Combining both of them, the extremely high enhancement of Ag@MIPs could be more rationalized by the synergetic effect of the “gate effect” and “dummy hot spots”. However, The deep insight into MIPs related SERS enhancement mechanism need to be further explored in future work.

Conclusions

In summery, we have successfully synthesized a Ag@MIPs hybrid system with a thin MIPs shell (~ 16 nm). As-prepared core-shell nanostructure shows a high sensitivity and selectivity toward template molecule. In this regard, it can be exactly interpreted by “gate effect” and “dummy hot spots”, or synergetic effect of both of them. However, there are many problems to handle before MIPs related SERS method could serve as a robust technique in practical applications. Therefore, future research efforts need to be continually made.

Acknowledgements

The authors would like to thank the financial support from the National Natural Science Foundation of China (No. 21176052 and 51379052), and the State Key Laboratory of Urban Water Resource and Environment, Harbin Institute of Technology (2013TS05).

Notes and references

^a Department of Chemistry, Harbin Institute of Technology, Harbin 150001, PR China.

^b State Key Lab of Urban Water Resource and Environment, Harbin Institute of Technology, Harbin 150090, PR China.

E-mail: lixin@hit.edu.cn;

The authors declare no competing financial interest.

Electronic Supplementary Information (ESI) available: See DOI: 10.1039/b000000x/

1. M. Fleischmann, P. J. Hendra and A. J. McQuillan, *Chem. Phys. Lett.*, 1974, **26**, 163-166.
2. M. Fan, G. F. S. Andrade and A. G. Brolo, *Anal. Chim. Acta*, 2011, **693**, 7-25.
3. K. Kneipp, Y. Wang, H. Kneipp, L. T. Perelman, I. Itzkan, R. Dasari and M. S. Feld, *Phys. Rev. Lett.*, 1997, **78**, 1667-1670.
4. S. M. Nie and S. R. Emery, *Science*, 1997, **275**, 1102-1106.
5. L. Brus, *Accounts Chem. Res.*, 2008, **41**, 1742-1749.
6. R. Zhang, Y. Zhang, Z. C. Dong, S. Jiang, C. Zhang, L. G. Chen, L. Zhang, Y. Liao, J. Aizpurua, Y. Luo, J. L. Yang and J. G. Hou, *Nature*, 2013, **498**, 82-86.
7. M. Harz, P. Rosch, K. D. Peschke, O. Ronneberger, H. Burkhardt and J. Popp, *Analyst*, 2005, **130**, 1543-1550.
8. M. Lin, L. He, J. Awika, L. Yang, D. R. Ledoux, H. Li and A. Mustapha, *J. Food Sci.*, 2008, **73**, T129-T134.
9. S. L. Truong, G. Levi, F. Bozon-Verduraz, A. V. Petrovskaya, A. V. Simakina and G. A. Shafeev, *Appl. Phys. A-Mater.*, 2007, **89**, 373-376.
10. X. Wang, C. Wang, L. Cheng, S.-T. Lee and Z. Liu, *J. Am. Chem. Soc.*, 2012, **134**, 7414-7422.
11. L. Xu, H. Kuang, C. Xu, W. Ma, L. Wang and N. A. Kotov, *J. Am. Chem. Soc.*, 2012, **134**, 1699-1709.
12. W. Ren, Y. Fang and E. Wang, *ACS Nano*, 2011, **5**, 6425-6433.
13. M. P. Cecchini, V. A. Turek, J. Paget, A. A. Kornyshev and J. B. Edel, *Nat. Mater.*, 2013, **12**, 165-171.
14. F. De Angelis, F. Gentile, F. Mecarini, G. Das, M. Moretti, P. Candeloro, M. L. Coluccio, G. Cojoc, A. Accardo, C. Liberale, R. P. Zaccaria, G. Perozziello, L. Tirinato, A. Toma, G. Cuda, R. Cingolani and E. Di Fabrizio, *Nat. Photonics*, 2011, **5**, 683-688.
15. X. Liu, L. Cao, W. Song, K. Ai and L. Lu, *ACS Appl. Mater. Inter.*, 2011, **3**, 2944-2952.
16. S. M. Ansar, R. Haputhanthri, B. Edmonds, D. Liu, L. Yu, A. Sygula and D. Zhang, *J. Phys. Chem. C*, 2011, **115**, 653-660.
17. R. A. Alvarez-Puebla and L. M. Liz-Marzan, *Chem. Soc. Rev.*, 2012, **41**, 43-51.
18. Y. Wang, B. Yan and L. Chen, *Chem. Rev.*, 2013, **113**, 1391-1428.
19. F. Lai, U. A. Orom, M. Cesaroni, M. Beringer, D. J. Taatjes, G. A. Blobel and R. Shiekhattar, *Nature*, 2013, **494**, 497-501.
20. C. Malitesta, E. Mazzotta, R. A. Picca, A. Poma, I. Chianella and S. A. Piletsky, *Anal. Bioanal. Chem.*, 2012, **402**, 1827-1846.
21. A. P. F. Turner, *Chem. Soc. Rev.*, 2013, **42**, 3184-3196.
22. X. Xing, S. Liu, J. Yu, W. Lian and J. Huang, *Biosens. Bioelectron.*, 2012, **31**, 277-283.
23. Y. Hoshino, H. Koide, T. Urakami, H. Kanazawa, T. Kodama, N. Oku and K. J. Shea, *J. Am. Chem. Soc.*, 2010, **132**, 6644-+.
24. E. L. Holthoff, D. N. Stratis-Cullum and M. E. Hankus, *Sensors*, 2011, **11**, 2700-2714.
25. P. Liu, R. Liu, G. Guan, C. Jiang, S. Wang and Z. Zhang, *Analyst*, 2011, **136**, 4152-4158.
26. J. Q. Xue, D. W. Li, L. L. Qu and Y. T. Long, *Anal. Chim. Acta.*, 2013, **777**, 57-62.
27. C. Limin, D. Yan and L. Xin, *Biosens. Bioelectron.*, 2013, **50**, 106-110.
28. B. Zhang, P. Xu, X. Xie, H. Wei, Z. Li, N. H. Mack, X. Han, H. Xu and H. L. Wang, *J. Mater. Chem.*, 2011, **21**, 2495-2501.
29. H. Liang, Z. Li, W. Wang, Y. Wu and H. Xu, *Adv. Mater.*, 2009, **21**, 4614-4618.
30. J. A. Dieringer, A. D. McFarland, N. C. Shah, D. A. Stuart, A. V. Whitney, C. R. Yonzon, M. A. Young, X. Y. Zhang and R. P. Van Duyne, *Faraday Discuss.*, 2006, **132**, 9-26.
31. D. Li, S. Wu, Q. Wang, Y. Wu, W. Peng and L. Pan, *J. Phys. Chem. C*, 2012, **116**, 12283-12294.
32. X. Zhu, L. Shi, M. S. Schmidt, A. Boisen, O. Hansen, J. Zi, S. Xiao and N. A. Mortensen, *Nano Lett.*, 2013, **13**, 4690-4696.
33. J. T. Bahns, Q. Guo, J. M. Montgomery, S. K. Gray, H. M. Jaeger and L. Chen, *J. Phys. Chem. C*, 2009, **113**, 11190-11197.
34. X. Li, H. Hu, D. Li, Z. Shen, Q. Xiong, S. Li and H. J. Fan, *ACS Appl. Mater. Inter.*, 2012, **4**, 2180-2185.
35. Y. Chen, M. B. O'Donoghue, Y. F. Huang, H. Kang, J. A. Phillips, X. Chen, M. C. Estevez, C. J. Yang and W. Tan, *J. Am. Chem. Soc.*, 2010, **132**, 16559-16570.
36. Y. Yoshimi, K. Sato, M. Ohshima and E. Piletska, *Analyst*, 2013, **138**, 5121-5128.
37. S. A. Piletsky, T. L. Panasyuk, E. V. Piletskaya, I. A. Nicholls and M. Ulbricht, *J. Membrane Sci.*, 1999, **157**, 263-278.
38. Y. Yoshimi, A. Narimatsu, K. Nakayama, S. Sekine, K. Hattori and K. Sakai, *J. Artif. Organs.*, 2009, **12**, 264-270.
39. <http://phys.org/news/2013-05-helicopter-light-beams-tool-quantum-optics.html>